Organic Electronics 13 (2012) 290–296

Contents lists available at SciVerse ScienceDirect

Organic Electronics

journal homepage: www.elsevier.com/locate/orgel

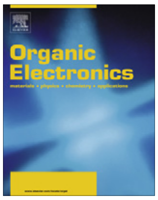

Molecular doping of low-bandgap-polymer:fullerene solar cells: Effects on transport and solar cells

Ali Veysel Tunc [a], Antonietta De Sio [a], Daniel Riedel [b], Felix Deschler [b], Enrico Da Como [b], Jürgen Parisi [a], Elizabeth von Hauff [a,*]

[a] *Energy and Semiconductor Research Laboratory, Institute of Physics, Carl von Ossietzky Universität Oldenburg, Oldenburg 26111, Germany*
[b] *Photonics and Optoelectronics Group, Department of Physics, CeNS Ludwig-Maximilians-Universität München, Munich 80799, Germany*

ARTICLE INFO

Article history:
Received 17 May 2011
Received in revised form 22 November 2011
Accepted 23 November 2011
Available online 7 December 2011

Keywords:
Photovoltaics
Organic semiconductors
Doping
Conducting polymer
Solar cells
Carrier mobility

ABSTRACT

We show how molecular doping can be implemented to improve the performance of solution processed bulk heterojunction solar cells based on a low-bandgap polymer mixed with a fullerene derivative. The molecular dopant 2,3,5,6-tetrafluoro-7,7,8,8-tetracyanoquinodimethane (F4-TCNQ) is introduced into blends of poly[2,6(4,4-bis-(2-ethylhexyl)-4H-cyclopenta[2,1-b:3,4-b0]-dithiophene)-alt-4,7-(2,1,3-benzothiadiazole)] (PCPDTBT) and [6,6]-phenyl-C61-butyric acid methyl ester (PCBM) via co-solution in a range of concentrations from 0% to 1%. We demonstrate that the hole conductivity and mobility increase with doping concentration using field-effect measurements. Photoinduced absorption (PIA) spectroscopy reveals that the polaron density in the blends increases with doping. We show that the open circuit voltage and short circuit current of the corresponding solar cells can be improved by doping at 0.5%, resulting in improved power conversion efficiencies. The increase in performance is discussed in terms of trap filling due to the increased carrier density, and reduced recombination correlated to the improvement in mobility.

1. Introduction

Solar cells based on polymer:fullerene bulk-heterojunctions (BHJ) can be processed from solution at low temperatures and low production costs to offer a promising technology for flexible, large area photovoltaic applications [1,2]. In the BHJ solar cell [3], the polymer and fullerene form an interpenetrated network of donor and acceptor domains at the nanoscale [4,5]. Excitons are generated upon light absorption by the polymer. The fullerene is used as an electron acceptor, and charge transfer occurs when excitons diffuse to the polymer and fullerene interface. An efficient collection of the photogenerated charge carriers depends on the percolation of holes and electrons towards the anode and cathode with minimized recombination. However, in such thin-film solar cells recombination is a delicate interplay between morphology and carrier lifetime/mobility [6–8]. Several aspects have been explored towards the optimization of morphology [9–11], whereas intrinsic carrier mobility is a material parameter, with limited possibilities for improvement [12]. Both the morphology of the active layer and the charge carrier mobilities in the blend influence the efficiency of BHJ solar cells, which is primarily limited by low photocurrents. The design of conjugated polymers with low bandgaps lying in the near infrared has improved the light harvesting properties and thus the amount of photocarriers potentially capable of generating photocurrent [13]. These novel low bandgap polymers have recently been the focus of intense research [13–15]. However, poor carrier transport

---

* Corresponding author. Present address: Institute of Physics, Albert-Ludwigs University of Freiburg, Freiburg 79104, Germany. Tel.: +49 (0)441 7983933; fax: +49 (0)441 7983990.

E-mail address: elizabeth.von.hauff@physik.uni-freiburg.de (E. von Hauff).

1566-1199/$ - see front matter © 2011 Elsevier B.V. All rights reserved.
doi:10.1016/j.orgel.2011.11.014

characteristics and the resulting recombination losses may remain a significant problem for further optimization [16].

PCPDTBT is a low bandgap polymer based on two alternating repeat units with different electro affinities, in this case dithiophene and benzothiadiazole [17]. PCPDTBT blended with the soluble fullerene derivative PCBM is considered to be a promising material combination for BHJ solar cells [18]. The power conversion efficiencies of these cells have been found to be limited by recombination resulting in relatively low short circuit currents (J_{sc}), fill factors (FF) and thus external quantum efficiencies (EQE) [16]. Previous studies addressing recombination effects in this system have been focussed on the role of morphology [19], and the transport properties of the blends [16]. While control over morphology has been effectively achieved by using solvent additives [20], the tuning of the transport characteristics remains more challenging.

Molecular doping is an effective possibility to improve the electrical characteristics of organic semiconductor devices [21]. Doping molecules with suitable energy levels can accept electrons from the highest occupied molecular orbital (HOMO) level of polymers, resulting in p-type doping in the ground state. F4-TCNQ is commonly used to p-dope organic semiconductors [21,22]. In small molecule devices, where stacked layers are prepared by sublimation, it has been shown that transport layers doped with F4-TCNQ can be used to lower the operating voltages of organic light emitting diodes (OLEDs) [23] and achieve efficient p–i–n junction solar cells [24]. Several investigations demonstrated how doping in such devices has an impact on carrier injection and extraction by modifying energy barriers at the metal organic interface [25,26]. On the other hand, many comprehensive studies on conjugated polymers mixed via co-solution with F4-TCNQ demonstrated that doping leads to an increase not only in conductivity but also in mobility, [27,28] so it is likely that doping may have an effect on the various recombination phenomena in BHJ solar cells. For example, the initial geminate recombination depends on the local mobilities of electrons and holes after charge transfer [29]. A very recent work from us based on transient absorption spectroscopy proved that it is possible to reduce geminate recombination in PCPDTBT:PCBM blend films upon doping [30]. An increased carrier mobility via doping was demonstrated by both diode and field-effect transistor (FET) measurements [27,28] resulting in the general improvement of the electrical properties in polymer films through doping. The improvement in transport has been recently attributed to the filling of traps by the dopant-induced carriers and a shift of the mobility edge towards the center of the density of states, where mobility is known to be higher [31].

In this paper, we show how molecular doping can be used to improve the hole mobility in solution processed blends based on PCPDTBT:PCBM and therefore the performance of BHJ solar cells. F4-TCNQ is introduced to the blend via co-solution at concentrations ranging from 0 to 1 wt.% with respect to the polymer, demonstrating a simple method to dope solution processed cells. From transport measurements based on FETs we demonstrate that the hole conductivity and mobility increase with doping concentration. Solar cells prepared with doped blends exhibit short circuit currents improved by more than 10%, resulting in higher power conversion efficiencies. We discuss the improvement in performance in terms of reduced recombination correlated to the increase in mobility and transport properties.

2. Material and methods

PCPDTBT, supplied by Konarka Technologies GmbH (Nürnberg, Germany), was p-doped with F4-TCNQ (Sigma-Aldrich) and blended with PCBM, purchased from Solenne BV. F4-TCNQ and PCPDTBT were separately dissolved in chlorobenzene, in concentrations of 1 mg/mL and 10 mg/mL, respectively. For the field-effect measurements, the dopant solution was added to the polymer solution to achieve concentrations of 0%; 0.1%; 0.2% and 0.3% by weight with respect to the polymer. Solutions were left stirring overnight. For the polymer:fullerene solutions, PCBM was added to obtain a weight ratio of 1:1 with respect to the polymer. The semiconducting layers were then spin coated onto pre-cleaned substrates. All solution processing was performed in a N_2-filled glovebox.

FETs were fabricated on highly n-doped silicon substrates purchased from Fraunhofer IPMS (Dresden) with a thermally grown layer of SiO_2 with a thickness of 230 ± 10 nm. The source-drain contacts are Au and have an interdigitated structure with channel lengths L of 20 μm and channel width W of 1 cm. The silicon substrates were cleaned using the same method as for the ITO substrates. The substrates were then transferred into the glove-box for deposition of the semiconductor via spin-coating. The electrical characterization of the transistors was carried out in a cryostat at 10^{-6} mbar in the dark. The source-drain current voltage characteristics were recorded using a Keithley 236 and the gate voltage was regulated with a Keithley 2400 source measurement unit.

For the PIA and solar cell measurements, blend solutions in chlorobenzene:diodooctane (100:3 v/v) and toluene:diodooctane (100:1 v/v), respectively, with a 1:2 polymer:fullerene ratio were prepared with doping concentrations from 0% to 1%. For the PIA measurements, the blends were spun onto saphire samples. The samples were excited at 660 nm and probed with white light from a halogen lamp. Laser induced changes in transmission of the white light source were measured using lock-in detection. The samples were cooled to 80 K and kept in vacuum during the measurements. To prepare solar cells, patterned ITO coated glass substrates from PGO (Germany) were cleaned in hot acetone and isopropanol and exposed for 10 min to an oxygen plasma treatment to remove organic residuals from the surface. PEDOT:PSS (HC Stark) was then spun on the substrates and annealed at 180 °C for 10 min. The layer thickness was 60 nm. The samples were transferred into the glovebox to perform all subsequent processing steps. The blends were spun on top of the PEDOT:PSS layer to get an active layer thickness of 80 nm. Here, doping concentrations from 0% to 1% were used. The cathode was formed by thermal evaporation of LiF:A1. The active layer of the solar cells was defined by the overlap of the cathode and anode, and was approximately 0.15 cm^2. The exact area was measured under an optical microscope.

Current-voltage characteristics (IV) of the solar cells under simulated AM 1.5 G sun light were recorded with a Keithley 2400 source measurement unit. The reference solar spectrum was provided by a class A solar simulator (P.E.T. Inc.) calibrated with a reference silicon photodiode supplied by Fraunhofer ISE (Germany). External quantum efficiency (EQE) was measured with a lock-in technique on a setup equipped with a Xe–Hg tandem lamp using a two-grating monochromator. The incident photon flux was monitored with a calibrated silicon photodetector.

3. Results and discussion

3.1. Field-effect measurements on doped PCPDTBT and PCPDTBT:PCBM

The influence of doping on the dark hole conductivity and mobility of PCPDTBT and PCPDTBT:PCBM was investigated using FET measurements on the pure polymer and the polymer:fullerene blends. The doped PCPDTBT (without PCBM) was used as a reference system to investigate the effects of the molecular dopant on the polymer alone. PCPDTBT and PCPDTBT:PCBM blends were doped with F4-TCNQ at concentrations of 0%; 0.1%; 0.2% and 0.3% with respect to the polymer. FETs were prepared according to the details provided in the experimental section.

We observe an increase in the source–drain current (I_{ds}) with doping concentration for both the pure polymer and the blend. This is shown in Fig. 1a, in which I_{ds} for a hole conducting channel (taken at a source–drain voltage (V_{ds}) of −10 V and a gate voltage (V_{gs}) of −60 V is plotted against the doping concentration for the pure polymer (black symbols) and the blend (red symbols). Besides the increase in the hole current when PCBM is added to the polymer by a factor of thirty, already discussed in previous reports [32], the current is observed generally to increase with doping, as a result of the increase in the *conductivity* of the polymer. While the improved conductivity in blends with respect to PCPDTBT can be attributed to changes in the polymer morphology due to PCBM, the trend observed with doping demonstrates the effect of F4-TCNQ in increasing the hole density, i.e. the p-type doping, in both systems. The increase in conductivity of the layer with doping concentration results in an increase in I_{ds} by more than an order of magnitude in the pure polymer going from 0 doping to 0.3% doping, and by a factor of four in the blends for the same doping range.

More interesting is the influence of the dopant on the charge carrier *mobility*. The hole field-effect mobility was determined from the linear part of the FET transfer characteristics according to ref. [33] for all the samples discussed in panel **a**. The mobility vs. doping concentration is shown in Fig. 1b for PCPDTBT (black symbols) and for PCPDTBT:PCBM blends (red symbols). These results clearly indicate that molecular doping can increase the hole mobility in PCPDTBT and PCPDTBT:PCBM blends. The mobility was observed to increase by a factor of *five* in the polymer from 0% to 0.3% doping and by a factor of *three* in the case of the blend. The increase in mobility is significant at 0.1% and begins to saturate between 0.2% and 0.3%, thus higher concentrations were not investigated. In addition, the increase in conductivity of the blends with doping leads to a decrease in the quality of the field effect behavior of the devices. This is consistent with results from the literature which demonstrated an increase in hole mobility

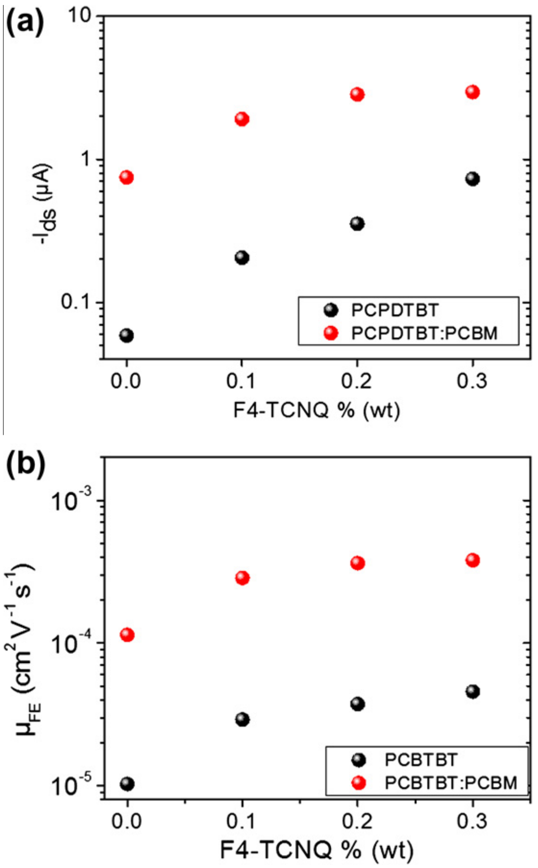

Fig. 1. FET parameters: (a) source–drain current I_{ds} at V_{ds} = −10 V and V_g = −60 V as a function of F4-TCNQ concentration for PCPDTBT (black squares) and PCPDTBT:PCBM (red dots) thin films. (b) Field-effect mobility extracted from the linear regime as a function of F4-TCNQ for the same samples in (a).

Table 1
Field-effect parameters of FET prepared with PCPDTBT and PCPDTBT:PCBM blends at doping concentrations of 0; 0.1; 0.2; and 0.3 wt.% with respect to the polymer.

	μ (cm^{2}V^{-1}s^{-1})	I_{on}/I_{off}	V_T (V)
PCPDTBT	1.03×10^{-5}	2×10^5	−32
PCPDTBT – F4-TCNQ (0.1%)	2.91×10^{-5}	1×10^3	5
PCPDTBT – F4-TCNQ (0.2%)	3.74×10^{-5}	2×10^1	20
PCPDTBT – F4-TCNQ (0.3%)	4.57×10^{-5}	4×10^0	–
PCPDTBT:PCBM	1.14×10^{-4}	5×10^4	0
PCPDTBT:PCBM – F4-TCNQ(0.1%)	2.86×10^{-4}	2×10^5	1
PCPDTBT:PCBM – F4-TCNQ(0.2%)	3.63×10^{-4}	1×10^4	5
PCPDTBT:PCBM – F4-TCNQ(0.3%)	3.80×10^{-4}	1×10^4	7

for polythiophene doped at F4-TCNQ concentrations similar to those reported here [34].

The FET parameters are summarized in Table 1. The on/off ratio and the threshold voltage (V_T) decrease with doping in both PCPDTBT and in the blend. This can be attributed to an improvement in the charge carrier injection due to doping and to a filling of the traps in the organic layer by the increased charge carrier concentration. The improved injection is consistent with reports showing that the injection barrier between Au and organic semiconductors can be lowered by doping with F4-TCNQ [35]. In addition, the high concentration of holes in the doped layers can lead to trap filling and a transition from a semiconductor- to a metallic-like behaviour. This effect can be seen specifically in the decrease of V_T with doping in the transfer characteristics of Fig. 2. Here, the transfer characteristics of the polymer and blends are plotted taking the linear part of the output curves at $V_{ds} = -10$ V. The threshold voltage, which corresponds to the onset for current in the channel of the FET [33], exhibits a significant shift. We can consider this as the voltage at which traps are filled and conduction begins. A similar behaviour has been recently reported for doped pentacene FETs [36]. Therefore, these results indicate the beneficial role of doping in increasing mobility by filling tail states in the polymer and in enabling better injection characteristics. The differences in the relative improvements of mobility and conductivity for the pure polymer and the blend with PCBM can be partially understood considering a dilution by a factor of two in the dopant density when going from PCPDTBT to PCPDTBT:PCBM. Below we discuss the negligible influence of dopant molecules on film morphology.

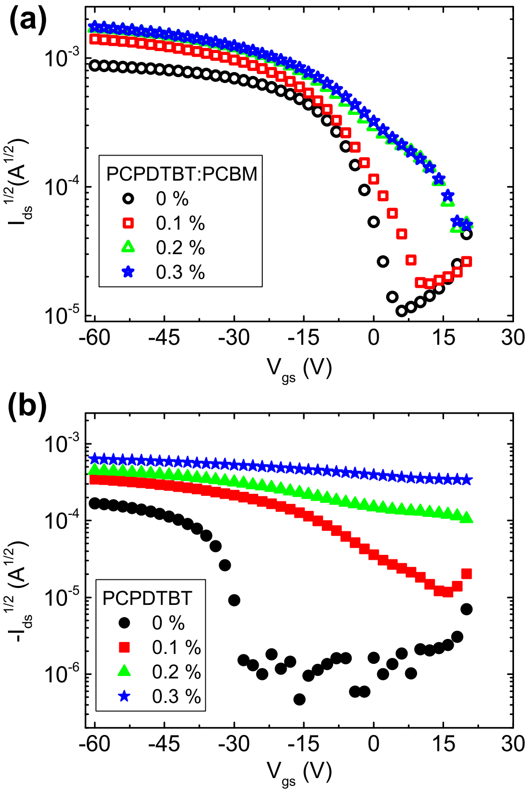

Fig. 2. Transfer characteristics (square root of source–drain current I_{ds} versus gate voltage V_{gs}) at $V_{ds} = -10$ V for PCPDTBT (a) and PCPDTBT:PCBM (b) FETs prepared with 0% (black crosses), 0.1% (red squares), 0.2% (green circles) and 0.3% (blue triangles) F4-TCNQ wt with respect to the polymer. (For interpretation of the references to color in this figure legend, the reader is referred to the web version of this article.)

Improvements in the hole mobility are expected to have an impact on the photocurrent in BHJ solar cells, for example on the initial geminate recombination of bound pairs at the polymer:fullerene interface. Such pairs are known to form *charge transfer excitons* at the heterojunction or separate into free carriers depending on the local mobility within the polymer and fullerene domains [29]. This geminate recombination has been directly correlated to the J_{sc} and a decrease in this recombination channel is expected to result in larger photocurrents. [29,37] In the next part of this study we examine the influence of the dopant on the polaron densities in the blend; polarons are the optical signatures of separated charge carriers.

3.2. Photoinduced absorption spectroscopy on PCPDTBT:PCBM blends doped with F4-TCNQ

We investigated the influence of the dopant on the excited states in the blends using steady-state photoinduced absorption spectroscopy (PIA). Fig. 3 shows the PIA spectra of the blends for doping concentrations from 0% to 1%. The spectra were corrected to account for the number of absorbed photons from the pump at 660 nm by normalizing with respect to the peak in the ground state bleaching (GSB) band, as this is equal for all samples excited under the same conditions. The spectrum of the undoped blend agrees with results from the literature, and the peaks at 0.93 eV and 1.42 eV correspond to polaron transitions [19]. Notable is the influence of the dopant on the polaron signals and on the position of the GSB onset at around 1.45 eV. At 0.93 eV the blend with 0.5% doping shows the highest intensity in the polaron signal. This intensity can be directly correlated to the polaron density. Differences between the polaron densities in the other blends are also

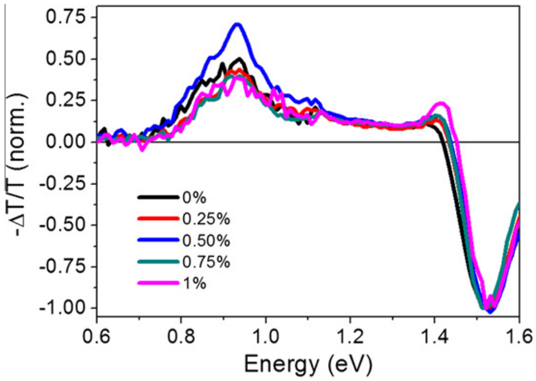

Fig. 3. PIA spectra of the PCPDTBT:PCBM blends for doping concentrations between 0% and 1%. Polaronic transistions can be seen at 0.93 eV and 1.42 eV. The positive signal at energies above 1.5 eV corresponds to ground state bleaching (GSB). The spectra were corrected for absorption by normalizing the GSB.

expected [30], but seem to be not apparent at the long time scales in steady-state experiments. Additionally, it can be observed that the GSB band shifts to higher energies with increasing doping concentrations. These results indicate that the tail states of the polymer are filled with the additional charge carriers from the dopant, which shifts the emissive recombination of carriers to higher energies in agreement with our previous results on photoluminescence [30]. This is also consistent with the increase in the mobility with doping observed in the field-effect measurements.

3.3. PCPDTBT:PCBM solar cells doped with F4-TCNQ

Fig. 4 shows the current density–voltage (*J*–*V*) characteristics of PCPDTBT:PCBM solar cells under illumination of AM 1.5 prepared with doping concentrations as specified in the figure. From the *J*–*V* characteristics an increase in the short circuit current density (J_{sc}) from 9.42 mA/cm^2 to 10.31 mA/cm^2 in the 0.5% doped blends is clearly apparent. The fill factor (FF) shows negligible differences going from 56% in the undoped cell (0%) to 55.4.% in the 0.5% doped cell, but the improvement in the J_{sc} (9 %) and the increase in V_{oc} (from 0.61 to 0.63 V) results in an overall increase in the efficiency, as detailed below. The inset shows the dark *JV* characteristics of the devices. The current density increases upon doping. These results agree with the FET measurements, which demonstrated saturation in the conductivity and mobility values at doping concentrations at doping concentrations around 0.3 %. Interestingly, in the case of the illuminated *JV*, the current continues to increase even at higher doping concentrations demonstrating the positive impact of doping on efficient charge separation, and the subsequent influence on the photocurrent and device efficiency.

Fig. 5 shows the external quantum efficiency (EQE) spectra of the solar cells. In general, the EQE exhibits two main features: one centred at 750 nm and the other at 370 nm. While the near infrared band (750 nm) can be assigned to photocurrent originating from the PCPDTBT absorption, the UV band is likely due to a superposition of PCBM and PCPDTBT contributions. The inset shows an absorption spectrum of the undoped blend as reference. With the introduction of the dopant in the polymer–fullerene system, the near IR EQE contribution due to PCPDTBT undergoes a visible enhancement for doping concentrations above 0.1%. This indicates that the collection of photogenerated charges is more efficient in a spectral region where PCPDTBT is the main absorber of light in the blend system. In general the data for the EQE reflect the trends in the *J*–*V* characteristics of the cells at J_{sc}.

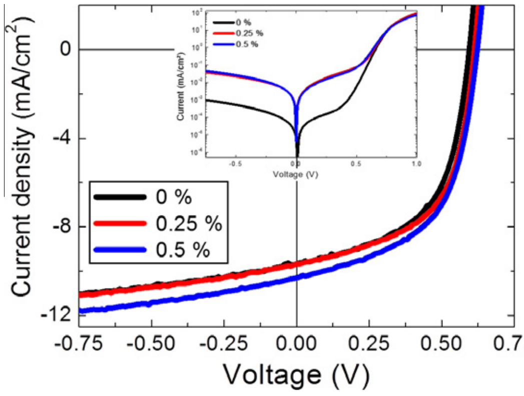

Fig. 4. *J*–*V* curves recorded under illumination with an AM 1.5 solar simulator for PCPDTBT:PCBM (1:1) solar cells doped with different amounts of F4-TCNQ: 0 (black), 0.25 (red), and 0.5 (blue). The insert shows the dark *JV* characteristics of the devices. (For interpretation of the references to color in this figure legend, the reader is referred to the web version of this article.)

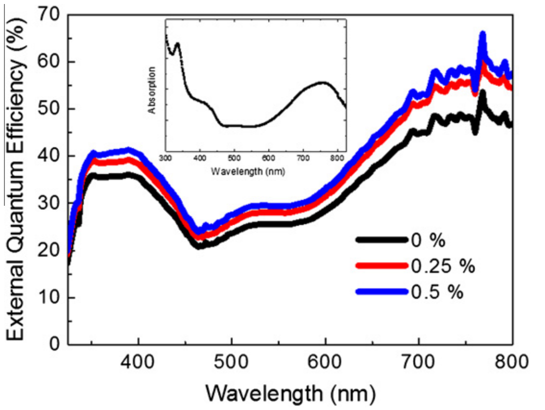

Fig. 5. EQE spectra for the solar cells shown in Fig. 4. The inset shows a typical absorption spectrum for a PCPDTBT:PCBM undoped blend.

To provide a better overview of the effect of doping on the solar cell performance the parameters extracted from the *J*–*V* characteristics are shown in Fig. 6. As already apparent from the *J*–*V* curves, it can be seen in panel **a** that J_{sc} increases with higher doping concentration as well as the open circuit voltage (panel **b**), for doping up to 0.5%. On the other hand, the FF (Fig. 6c) varies only slightly (decreasing by a factor of 0.12) with doping over the whole range investigated. Both the increase in J_{sc} and V_{oc} are signatures of a reduced recombination of the photogenerated carriers. As reported in studies on the nature of V_{oc} this de-

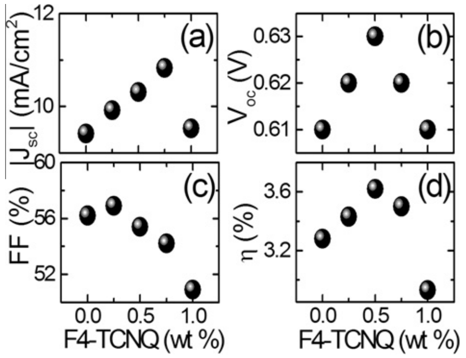

Fig. 6. Photovoltaic parameters extracted from the J-V characteristics of PCPDTBT:PCBM solar cells as a function of F4-TCNQ concentration in the blend. (a) Short circuit current; (b) open circuit voltage; (c) fill factor; and (d) power conversion efficiency.

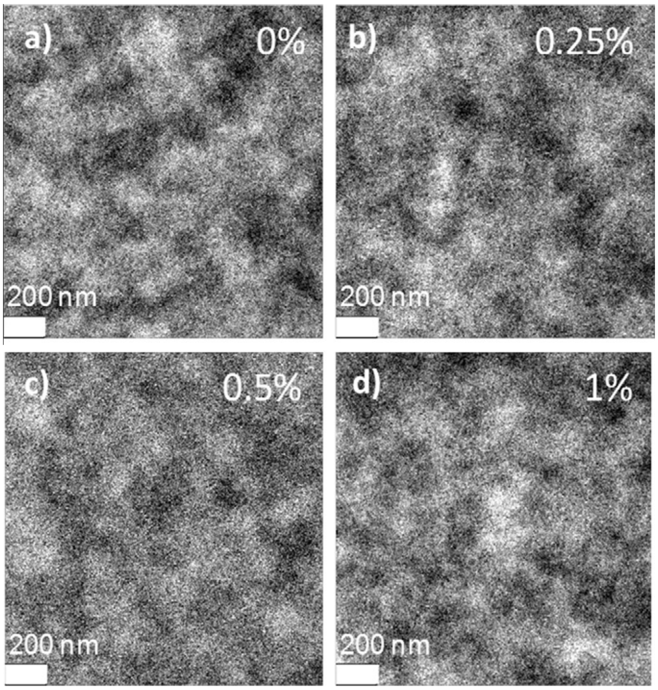

Fig. 7. Transmission electron microscopy images of PCPDTBT:PCBM blends for different concentration of F4-TCNQ. (a) 0%; (b) 0.25%; (c) 0.5%; and (d) 1%. The images were obtained with an operating voltage of 100 kV.

pends on the overall amount of carriers recombining via charge transfer excitons [38]. We demonstrated that doping can reduce the amount of carriers recombining as charge transfer excitons in blends of the same materials [30]. Therefore, the increase in the V_{oc} and J_{sc} can be directly correlated to reduced recombination in the doped cells. The increase in efficiency Fig. 6d) by a factor of 10% is essentially determined by the improvement in the J_{sc} with doping. Considering that the thicknesses of the blend films were all ~80 nm, resulting in optical absorption characteristics with negligible differences, the improvement in efficiency can be clearly attributed to a decrease in recombination and better charge carrier transport and extraction.

3.4. Morphology of the blend films

Fig. 7 shows transmission electron microscopy pictures of four BHJ films of PCPDTBT:PCBM doped with different amounts of F4-TCNQ. Several studies have already demonstrated how the bright/dark contrast of these images can be used to distinguish between polymer and fullerene rich domains [4,39]. PCBM rich domains appear as darker regions, while polymeric regions appear bright. The images clearly show the formation of PCBM domains with average in-plane dimensions of about 100 nm in diameter. The shape of the domains appears to be irregular with borders which are not well defined. An important aspect to be noted is that doping at these concentrations has no influence on the morphology of the BHJ. The four pictures are virtually identical and we exclude substantial effects due to morphology changes in the solar cell improvements reported in Fig. 4 upon doping.

4. Conclusions

We demonstrate that molecular doping using F4-TCNQ leads to an increase in the photocurrent in PCPDTBT:PCBM solar cells. We investigate blends doped at 0; 0.1; 0.25, 0.5 and 1 wt.% with respect to the polymer. Field-effect measurements demonstrate that doping increases the hole conductivity and mobility in both PCPDTBT films and PCPDTBT:PCBM blends. The conductivity of the pristine polymer increases by more than ten times and for the polymer:fullerene blend by about four upon doping. The hole mobility was also observed to increase with doping concentrations between 0% and 0.3% by five times for the pure polymer and three for the blend. PIA spectroscopy revealed an increase in the polaron densities and a shift in the GSB band, corresponding to trap filling by the increase in charges introduced by doping. In solar cells, doping leads to increases in the photocurrent from 9.42 to 10.31 mA/cm^2 and an overall increase in the solar cell efficiency from 3.28% to 3.62 %. From the EQE data it is apparent that doping increases the efficiency in collecting photogenerated charges in spectral regions attributed to the PCPDTBT absorption. These results show that molecular doping is a feasible and simple method to improve the efficiency of BHJ solar cells.

Acknowledgements

The authors gratefully acknowledge funding from the SPP1355 “Elementary Processes in Organic Photovoltaics” of the DFG. The Oldenburg Group additionally acknowledges funding from the EWE-Nachwuchsgruppe “Dünnschichtphotovoltaik” by the EWE AG Oldenburg.

References

[1] G. Dennler, M.C. Scharber, C.J. Brabec, Polymer–fullerene bulk-heterojunction solar cells, Advanced Materials 21 (2009) 1323–1338.

[2] R. Gaudiana, C. Brabec, Organic materials – fantastic plastic, Nature Photonics 2 (2008) 287–289.

[3] G. Yu, J. Gao, J.C. Hummelen, F. Wudl, A.J. Heeger, Polymer photovoltaic cells – enhanced efficiencies via a network of internal donor–acceptor heterojunctions, Science 270 (1995) 1789–1791.

[4] J.K.J. van Duren, X.N. Yang, J. Loos, C.W.T. Bulle-Lieuwma, A.B. Sieval, J.C. Hummelen, R.A.J. Janssen, Relating the morphology of poly(p-phenylene vinylene)/methanofullerene blends to solar-cell performance, Advanced Functional Materials 14 (2004) 425–434.

[5] H. Hoppe, M. Niggemann, C. Winder, J. Kraut, R. Hiesgen, A. Hinsch, D. Meissner, N.S. Sariciftci, Nanoscale morphology of conjugated polymer/fullerene-based bulk-heterojunction solar cells, Advanced Functional Materials 14 (2004) 1005–1011.

[6] P.W.M. Blom, V.D. Mihailetchi, L.J.A. Koster, D.E. Markov, Device physics of polymer: fullerene bulk heterojunction solar cells, Advanced Materials 19 (2007) 1551–1566.

[7] T.M. Clarke, J.R. Durrant, Charge photogeneration in organic solar cells, Chemical Reviews 110 (2010) 6736–6767.

[8] A. Pivrikas, G. Juscaronka, A.J. Mozer, M. Scharber, K. Arlauskas, N.S. Sariciftci, H. Stubb, R. Österbacka, Bimolecular recombination coefficient as a sensitive testing parameter for low-mobility solar-cell materials, Physical Review Letters 94 (2005) 176806.

[9] Y. Yao, J.H. Hou, Z. Xu, G. Li, Y. Yang, Effect of solvent mixture on the nanoscale phase separation in polymer solar cells, Advanced Functional Materials 18 (2008) 1783–1789.

[10] J.K. Lee, Ma. WL, C.J. Brabec, J. Yuen, J.S. Moon, J.Y. Kim, K. Lee, G.C. Bazan, A.J. Heeger, Processing additives for improved efficiency from bulk heterojunction solar cells, Journal of the American Chemical Society 130 (2008) 3619–3623.

[11] D. Chirvase, J. Parisi, J.C. Hummelen, V. Dyakonov, Influence of nanomorphology on the photovoltaic action of polymer–fullerene composites, Nanotechnology 15 (2004) 1317–1323.

[12] A. Salleo, R.J. Kline, D.M. DeLongchamp, M.L. Chabinyc, Microstructural characterization and charge transport in thin films of conjugated polymers, Advanced Materials 22 (2010) 3812–3838.

[13] H.Y. Chen, J.H. Hou, S.Q. Zhang, Y.Y. Liang, G.W. Yang, Y. Yang, Yu. LP, Y. Wu, G. Li, Polymer solar cells with enhanced open-circuit voltage and efficiency, Nature Photonics 3 (2009) 649–653.

[14] A. Dhanabalan, J.K.J. van Duren, P.A. van Hal, J.L.J. van Dongen, R.A.J. Janssen, Synthesis and characterization of a low bandgap conjugated polymer for bulk heterojunction photovoltaic cells, Advanced Functional Materials 11 (2001) 255–262.

[15] N. Blouin, A. Michaud, M. Leclerc, A low-bandgap poly(2,7-carbazole) derivative for use in high-performance solar cells, Advanced Materials 19 (2007) 2295–2300.

[16] M. Lenes, M. Morana, C.J. Brabec, P.W.M. Blom, Recombination-limited photocurrents in low bandgap polymer/fullerene solar cells, Advanced Functional Materials 19 (2009) 1106–1111.

[17] Z. Zhu, D. Waller, R. Gaudiana, M. Morana, D. Muhlbacher, M. Scharber, C. Brabec, Panchromatic conjugated polymers containing alternating donor/acceptor units for photovoltaic applications, Macromolecules 40 (2007) 1981–1986.

[18] D. Muhlbacher, M. Scharber, M. Morana, Z.G. Zhu, D. Waller, R. Gaudiana, C. Brabec, High photovoltaic performance of a low-bandgap polymer, Advanced Materials 18 (2006) 2884–2889.

[19] D. Di Nuzzo, A. Aguirre, M. Shahid, V.S. Gevaerts, S.C.J. Meskers, R.A.J. Janssen, Improved film morphology reduces charge carrier recombination into the triplet excited state in a small bandgap polymer-fullerene photovoltaic cell, Advanced Materials 22 (2010) 4321–4324.

[20] J. Peet, J.Y. Kim, N.E. Coates, Ma. WL, D. Moses, A.J. Heeger, G.C. Bazan, Efficiency enhancement in low-bandgap polymer solar cells by processing with alkane dithiols, Nature Materials 6 (2007) 497–500.

[21] K.H. Yim, G.L. Whiting, C.E. Murphy, J.J.M. Halls, J.H. Burroughes, R.H. Friend, J.S. Kim, Controlling electrical properties of conjugated polymers via a solution-based p-type doping, Advanced Materials 20 (2008) 3319–3324.

[22] K. Walzer, B. Maennig, M. Pfeiffer, K. Leo, Highly efficient organic devices based on electrically doped transport layers, Chemical Reviews 107 (2007) 1233–1271.

[23] J. Blochwitz, M. Pfeiffer, T. Fritz, K. Leo, Low voltage organic light emitting diodes featuring doped phthalocyanine as hole transport material, Applied Physics Letters 73 (1998) 729–731.

[24] C. Falkenberg, C. Uhrich, S. Olthof, B. Maennig, M.K. Riede, K. Leo, Efficient p–i–n type organic solar cells incorporating 1,4,5,8-naphthalenetetracarboxylic dianhydride as transparent electron transport material, Journal of Applied Physics 104 (2008) 034506.

[25] C.K. Chan, W. Zhao, A. Kahn, I.G. Hill, Influence of chemical doping on the performance of organic photovoltaic cells, Applied Physics Letters 94 (2009) 203306.

[26] W.Y. Gao, A. Kahn, Controlled p doping of the hole-transport molecular material N,N′-diphenyl-N,N′-bis(1-naphthyl)-1,1(′)-biphenyl-4, 4′-diamine with tetrafluorotetracyanoquinodimethane, Journal of Applied Physics 94 (2003) 359–366.

[27] Y. Zhang, B. de Boer, P.W.M. Blom, Controllable molecular doping and charge transport in solution-processed polymer semiconducting layers, Advanced Functional Materials 19 (2009) 1901–1905.

[28] Y.A. Zhang, P.W.M. Blom, Enhancement of the hole injection into regioregular poly(3-hexylthiophene) by molecular doping, Applied Physics Letters 97 (2010) 083303.

[29] D. Veldman, O. Ipek, S.C.J. Meskers, J. Sweelssen, M.M. Koetse, S.C. Veenstra, J.M. Kroon, S.S. van Bavel, J. Loos, R.A.J. Janssen, Compositional and electric field dependence of the dissociation of charge transfer excitons in alternating polyfluorene copolymer/fullerene blends, Journal of the American Chemical Society 130 (2008) 7721–7735.

[30] F. Deschler, E. Da Como, T. Limmer, R. Tautz, T. Godde, M. Bayer, E. von Hauff, S. Yilmaz, S. Allard, U. Scherf, J. Feldmann, Reduced charge transfer exciton recombination in organic semiconductor heterojunctions by molecular doping, Physical Review Letters 107 (2011) 127402.

[31] Y. Zhang, B. de Boer, P.W.M. Blom, Trap-free electron transport in poly(p-phenylene vinylene) by deactivation of traps with n-type doping, Physical Review B 81 (2010) 085201.

[32] S.M. Tuladhar, D. Poplavskyy, S.A. Choulis, J.R. Durrant, D.D.C. Bradley, J. Nelson, Ambipolar charge transport in films of methanofullerene and poly(phenylenevinylene)/methanofullerene blends, Advanced Functional Materials 15 (2005) 1171–1182.

[33] G. Horowitz, Organic field-effect transistors, Advanced Materials 10 (1998) 365–377.

[34] L. Ma, W.H. Lee, Y.D. Park, J.S. Kim, H.S. Lee, K. Choa, High performance polythiophene thin-film transistors doped with very small amounts of an electron acceptor, Applied Physics Letters 92 (2008) 063310.

[35] N. Koch, S. Duhm, J.P. Rabe, A. Vollmer, R.L. Johnson, Optimized hole injection with strong electron acceptors at organic-metal interfaces, Physical Review Letters 95 (2005) 237601.

[36] W. Zhao, Y.B. Qi, T. Sajoto, S. Barlow, S.R. Marder, A. Kahn, Remote doping of a pentacene transistor: control of charge transfer by molecular-level engineering, Applied Physics Letters 97 (2010) 3.

[37] M. Hallermann, E. Da Como, J. Feldmann, M. Izquierdo, S. Filippone, N. Martin, S. Juchter, E. von Hauff, Correlation between charge transfer exciton recombination and photocurrent in polymer/fullerene solar cells, Applied Physics Letters 97 (2010) 023301.

[38] K. Vandewal, K. Tvingstedt, A. Gadisa, O. Inganäs, J.V. Manca, On the origin of the open-circuit voltage of polymer–fullerene solar cells, Nature Materials 8 (2009) 904–909.

[39] M. Hallermann, I. Kriegel, E. Da Como, J.M. Berger, E. von Hauff, J. Feldmann, Charge transfer excitons in polymer/fullerene blends: the role of morphology and polymer chain conformation, Advanced Functional Materials 19 (2009) 3662–3668.